Journal of Computational Physics 510 (2024) 112980

Contents lists available at ScienceDirect

Journal of Computational Physics

journal homepage: www.elsevier.com/locate/jcp

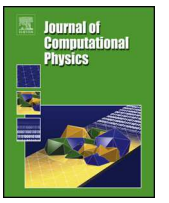

Multicontinuum homogenization. General theory and applications

E. Chung [a], Y. Efendiev [b,*], J. Galvis [c], W.T. Leung [d]

[a] Department of Mathematics, The Chinese University of Hong Kong, Sha Tin, Hong Kong
[b] Department of Mathematics, Texas A&M University, College Station, TX 77843, USA
[c] Departamento de Matemáticas, Universidad Nacional de Colombia, Carrera 45 No. 26-85, Edificio Uriel Gutiérrez, Bogotá D.C., Colombia
[d] Department of Mathematics, City University of Hong Kong, Hong Kong

ARTICLE INFO

Keywords:
Multiscale
Upscaling
Multicontinuum
Homogenization
Mixture theory
Porous media

ABSTRACT

In this paper, we discuss a general framework for multicontinuum homogenization. Multicontinuum models are widely used in many applications and some derivations for these models are established. In these models, several macroscopic variables at each macroscale point are defined and the resulting multicontinuum equations are formulated. In this paper, we propose a general formulation and associated ingredients that allow performing multicontinuum homogenization. Our derivation consists of several main parts. In the first part, we propose a general expansion, where the solution is expressed via the product of multiple macro variables and associated cell problems. The second part consists of formulating the cell problems. The cell problems are formulated as saddle point problems with constraints for each continua. Defining the continua via test functions, we set the constraints as an integral representation. Finally, substituting the expansion to the original system, we obtain multicontinuum systems. We present an application to the mixed formulation of elliptic equations. This is a challenging system as the system does not have symmetry. We discuss the local problems and various macroscale representations for the solution and its gradient. Using various order approximations, one can obtain different systems of equations. We discuss the applicability of multicontinuum homogenization and relate this to high contrast in the cell problem. Numerical results are presented.

1. Introduction

Many problems have multiscale nature. For example, the flow in porous media occurs in multiscale media with heterogeneities at multiple scales and high contrast. The simulations of these problems are often performed on a coarse computational grid, where the grid size is much larger compared to the scales of heterogeneities. In these simulations, we distinguish two cases in the paper. The first is the case with no-scale separation and the second is the case with scale separation. In the first case, approaches use the information within the entire computational grid or beyond to derive macroscopic equations. We will not discuss this case in the paper. In the second case, the representative volume-based information (which is much smaller compared to the target coarse block) is used in deriving macroscopic equations.

For the case of no-scale separation, many approaches are developed to account for subgrid effects. These approaches, e.g., [17,20,21,24,26,18,29,6,23,16,19,2,1], include the construction of multiscale basis functions that are supported in domain larger

* Corresponding author.
E-mail address: yalchinrefendiev@gmail.com (Y. Efendiev).

https://doi.org/10.1016/j.jcp.2024.112980
Received 15 September 2023; Received in revised form 7 February 2024; Accepted 28 March 2024

Available online 18 April 2024

than the target coarse block. Among these approaches, the CEM-GMsFEM [18] is related to the approaches presented in this paper. In these approaches, the multiscale basis functions are computed in oversampled regions. There are several basis functions in each target coarse block representing different continua effects. These concepts will further be used in multicontinua homogenization.

In the case of scale separation, one uses information in representative volume (which is much smaller compared to the coarse block) to derive effective properties. The well-known approach includes the homogenization technique [11,12,8,4], which is widely used in many applications. The main idea of this approach is to assume that the solution in each macroscopic point, can be represented by its average. The homogenization method provides a systematic expansion, which allows for deriving the equations. In this derivation, the small-scale ϵ is the RVE size. In the derivation, all terms depending on different powers of ϵ are separated. The latter is one of the limitations in extending these methods to problems where the media properties can depend on ϵ (high-contrast case).

In this paper, we introduce a general homogenization method, where we assume that the media properties can have high contrast. In our expansion, we consider that each macroscopic point has several macroscopic variables associated with it. The macroscopic variables are defined via auxiliary functions and assumed to be smooth functions. The expansion of the solution via macroscopic variables uses the solution of local microscopic problems posed in RVE, called solutions of cell problems. These local problems account for the micro-scale behavior of the solution given certain constraints. These constraints are related to the definition of macroscopic variables. In particular, our first cell problem imposes constraints to represent the constants in the average behavior of each continua. The consequent cell problems impose constraints to represent the high-order polynomials in the average behavior of each continua.

The multi-continuum homogenization expansion is substituted into the fine-scale equations. Our next assumptions include the fact that the integrals in the macroscopic variational formulation can be written in terms of the integrals over RVE and macroscopic variables are smooth. Using these assumptions, we derive a system of equations on a coarse grid. The resulting system of equation include additional terms and can involve higher-order derivatives. These equations share similarities to other models derived earlier and some terms can be negligible due to high contrast in the media properties.

Our approaches share some common ingredients with mixture theories [30,33,28]. In mixture theories, the conservation of mass and momentum are written for each component. This model can be used in deriving a general set of macroscopic equations. However, these models do not make any specific assumptions on exchange terms. Our models generalize some earlier derived model equations related to works [22], dual-permeability models [31,9,32,3,25,14,7,10,15,5] and we establish a general tool for deriving multicontinuum homogenization models.

One of the challenging aspects of multicontinuum homogenization is in formulating cell problems correctly. We consider large oversampled regions, where we can impose higher-order polynomial constraints. By imposing averages in each RVE within the oversampled region, our main test is to guarantee that the solution of the cell problem converges to zero. To achieve this, one needs a careful formulation of cell problems. For example, in a carefully studied example of mixed Darcy equations, we show how one can achieve this. We obtain a generalized Darcy approximation on the coarse grid. We present an error analysis for our multicontinuum approach in a separate arxiv paper [27].

We present numerical examples. In this numerical example, we consider a mixed formulation between velocity and pressure in Darcy's equation. Because pressure and velocity are treated separately, their relation at the microscale will not necessarily preserve at the macroscale as in the standard homogenization. We note that there is a linear relation between the velocity and the gradient of the pressure via the multiscale permeability field. Because the mixed formulation is not symmetric, this causes further challenges that are addressed in numerical examples when imposing local constraint problems. Our numerical results show a good convergence as we decrease the mesh size.

The paper is organized as follows. In the next section, we present preliminaries and a simple derivation of multicontinuum homogenization for zero-order equations. In Section 3, we present a general theory for multicontinuum homogenization and also discuss the relation to mixture theory. Section 4 is devoted to mixed-order systems. In Section 5, we present numerical experiments.

2. Preliminaries and zero order equation

To present preliminaries, we consider zero-order equations (following [12]). We consider the following zero-order equation

$$A(x)u(x) = f(x), \tag{1}$$

where $A(x)$ is a scalar function with multiple scales and high contrast. For example, we assume A is a periodic function where the period consists of two distinct regions with highly varying coefficients. We denote by ψ_i the characteristic function for the region i, called the ith continua.

It is assumed that the problem is solved on a computational grid consisting of grid blocks, denoted ω, that are much larger than heterogeneities. We assume some type of periodicity within each computational block represented by Representative Volume Element R_ω that corresponds to a computational element ω (see Fig. 1) (more precise meaning will be defined later). We assume that within each R_ω, there are several distinct average states (known as multicontinua). We denote the characteristic function for the continuum i within R_ω by ψ_i^ω (ω will be omitted since local computations are restricted to a coarse block), i.e., $\psi_i = 1$ within continuum i (can be irregularly shaped regions consisting of several parts, in general) and 0 otherwise. We introduce oversampled R_ω^+ that contains several R_ω^p's, where p denotes different R_ω's. We denote the central (target) RVE by, simply, R_ω. We denote ψ_i^p, the characteristic function for R_ω^p and will omit the index p for simplicity if it is clear which region we are referring to.

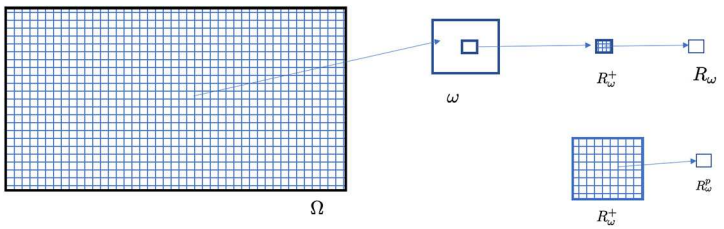

Fig. 1. Illustration.

We consider the expansion of u in each RVE as (for simplicity, we use equal sign instead of approximation)

$$u = \phi_i U_i, \tag{2}$$

where ϕ_i is a microscopic function for each i and $U_i(x)$ is a smooth function for each i. The summation over repeated indices is taken. To obtain the microscopic function ϕ_i, we formulate the following cell problems in each RVE within ω and use y dependence to denote microscopic nature:

$$\begin{aligned} A(y)\phi_i(y) &= D_{ij}\psi_j \ \text{ in } R_\omega \\ \int_{R_\omega} \phi_i\psi_j &= \delta_{ij}\int_{R_\omega}\psi_j, \ \text{for each } j, \end{aligned} \tag{3}$$

where D_{ij} are constants and can be shown that $D_{ij}\psi_j = C_i\psi_i$. Moreover, it can be easily computed that

$$C_j = \frac{\int_{R_\omega}\psi_j}{\int_{R_\omega}\psi_j^2 A^{-1}}.$$

Next, we derive macroscopic equations. For this, we first write an integral form (for any test function v)

$$\begin{aligned} \int_D fv &= \int_D A(x)u(x)v(x) = \sum_\omega \int_\omega A(x)u(x)v(x) \\ &\approx \sum_\omega \frac{|\omega|}{|R_\omega|}\int_{R_\omega} A(y)u(y)v(y). \end{aligned} \tag{4}$$

Substituting u from (2) into the equation and writing $v = \phi_i V_i$, we get

$$\int_{R_\omega} A(y)u(y)v(x)dy \approx U_i(x_\omega)V_j(x_\omega)\int_{R_\omega} A(y)\phi_i(y)\phi_j(y)\,dy, \tag{5}$$

where x_ω is a mid-point of R_ω. We will omit the microscopic dependence of macroscale variables (e.g., U_i) and simply use U_i notation

$$\int_{R_\omega} A(y)u(y)v(x)dy = U_iV_j\int_{R_\omega} A(y)\phi_i(y)\phi_j(y)\,dy. \tag{6}$$

We denote

$$\alpha_{ij} = \int_{R_\omega} A(y)\phi_i(y)\phi_j(y)\,dy. \tag{7}$$

It can be shown that

$$\alpha_{ij} = \delta_{ij}C_i\int_{R_\omega}\psi_j. \tag{8}$$

From the above, we see that the macroscopic equation has the form

$$\alpha_{ij}U_i = b_j,$$

where

$$b_j = \int_{R_\omega} f\phi_j.$$

Taking into account that α is a diagonal matrix, we have

$$U_i = \frac{b_i}{C_i \int_{R_\omega} \psi_i}.$$

We note that, in single continua homogenization, we obtain

$$U_1 = b_1 \frac{1}{|R_\omega|^2} \int_{R_\omega} A^{-1}.$$

3. General case. A formal derivation

In this section, we present a formal derivation of generalized multicontinuum homogenization. The derivation makes several assumptions, which may or may not hold depending on particular problems. We will make these assumptions as we go along.

We consider a general linear system given by

$$\frac{\partial u}{\partial t} + Au = f, \text{ in } D, \tag{9}$$

where A is a differential operator, u is a vector valued solution and D is the domain. The problem (9) is supplemented with some appropriate initial and boundary conditions. We next present several examples.

Example 1. In the scalar case, $Au = -div(\kappa(x)\nabla u)$, where $\kappa(x)$ is a multiscale and high-contrast coefficient.

Example 2. In a vector case, one can consider the elasticity problem with $Au = -\nabla_i C_{ijkl}(x) e_{kl}(u)$, where $C_{ijkl}(x)$'s represent heterogeneous and high-contrast media properties, $e_{kl}(u) = (\nabla_k u_l + \nabla_l u_k)/2$, and u is the displacement vector.

Example 3. We can consider Example 1 in a mixed formulation as a first-order system. In this case, $u = (p, v)$, where p and v solve $\kappa^{-1} v + \nabla p = 0$, $div(v) = f$.

Example 4. One can consider the first order systems, $Au = v(x) \cdot \nabla u + a(x)u$, where $v(x)$ and $a(x)$ are highly heterogeneous fields.

We write (9) as a variational problem

$$(\frac{\partial u}{\partial t}, v) + a_D(u, v) = (f, v), \tag{10}$$

where $a_D(u, v) = \int_D (Au)v$, e.g., in Example 1, $a_D(u, v) = \int_D \kappa \nabla u \cdot \nabla v$ (assuming zero Dirichlet boundary conditions).

In the multicontinuum homogenization, we assume that in each RVE, R_ω, there exist functions ψ_i (i refers to continua, ψ_i can be a characteristic function of subregion), such that

$$U_i(x^*_\omega) = \frac{\int_{R_\omega} u\psi_i}{\int_{R_\omega} \psi_i}$$

are macroscopic variables, where x^*_ω is a point in R_ω. One main assumption is that U_i's are smooth functions if we consider them over all RVEs. In our examples, the macroscopic variables have physical meanings as they represent the average of the solution in subregions associated with ψ_i's. Next, we present the steps in deriving macroscopic equations.

Step 1. Expansion.

The first step consists of expanding the solution u in terms of macroscopic variables. The coefficients in front of them, denoted by ϕ_i's, represent the local microscopic solution in RVE. We consider the expansion of the solution u as

$$u = \phi_m U_m + \phi^j_m \nabla_j U_m + \phi^{ij}_m \nabla^2_{ij} U_m + ..., \tag{11}$$

where ∇_j refers to $\frac{\partial}{\partial x_j}$. In this expansion, we will discuss the functions ϕ, which are defined as the solutions of local problems in RVE, R_ω. We note that the number of macroscale variables defines the size of the coarse system. In general, we expect that the number of macroscale variables is small compared to the number of fine degrees of freedom.

Step 2. Cell problems.

Next, we introduce equations for ϕ_i's. These equations are written in each RVE subject to some constraints. These constraints are related to definitions of macroscopic variables. We use Taylor's expansion concepts in defining the local functions such that they solve local problems with constraints that their averages with respect to ψ_i behave as constants, linear functions, and quadratic functions.

Our first cell problem imposes constraints to represent the constants in the average behavior of each continua (continua m in (12)). We note that all cell problems are solved with zero Dirichlet boundary conditions. Because of oversampling region. We expect the boundary conditions do not affect the homogenized equations as described below. We consider the cell problem in oversampled regions R^+_ω that contain several R_ω, denoted by R^p_ω.

$$\begin{aligned} A\phi_m^i &= \Gamma_{mn}^{ijp}\psi_n^p e^j \text{ in } R_\omega^+, \\ \int_{R_\omega^p} \phi_m^i \psi_n^p &= \delta_{mn} e^i \int_{R_\omega^p} \psi_n^p, \ \forall p, \end{aligned} \tag{12}$$

where e^i is the unit vector (solution u is vector valued) and ψ_n^p is the characteristic function in R_ω^p. This cell problem corresponds to appropriate energy minimizing solution subject to the constraints. Here and later, by Γ, we denote the Lagrange multipliers due to constraints. We denote ϕ_m the matrix spanned by ϕ_m^i (as columns).

Our second cell problem imposes constraints to represent the linear functions in the average behavior of each continua.

$$\begin{aligned} A\phi_m^{il} &= \Gamma_{mn}^{ijpl}\psi_n^p e^j \text{ in } R_\omega^+, \\ \int_{R_\omega^p} \phi_m^{il} \psi_n^p &= \delta_{mn} e^i \int_{R_\omega^p} (x_l - c_l)\psi_n^p, \ \forall p, \end{aligned} \tag{13}$$

where c_l (later on also) is chosen such that $\int_{R_\omega}(x_l - c_l) = 0$, where R_ω is the RVE defined in the middle of R_ω^+. Similarly, we denote ϕ_m^l the matrix spanned by ϕ_m^{il} (as columns).

We can also define higher-order cell problems. The next cell problem imposes constraints to represent the quadratics in the average behavior of each continua.

$$\begin{aligned} A\phi_m^{ijl} &= \Gamma_{mn}^{ijlps}\psi_n^p e^s \text{ in } R_\omega^+, \\ \int_{R_\omega^p} \phi_m^{ijl} \psi_n^p &= \delta_{mn} e^i \int_{R_\omega^p} (x_j x_l - c_{jl})\psi_n^p, \ \forall p. \end{aligned} \tag{14}$$

Similarly, we denote ϕ_m^{lj} the matrix spanned by ϕ_m^{ijl} (as columns).

We note that in our cell problems, we solve for each component of the vector solutions. The first cell problem is scalar and the number of higher order cell problems depends on the dimension of the space. In some applications, one can lump some components if some relations between components of the vector are known apriori.

Existence and uniqueness can be shown in most cases for positive symmetric operators with appropriate norms. In general, we need inf-sup condition for well-posedness of cell problems [13]. We note that the local solution away from R_ω (middle RVE) is independent of the oversampling domain size. This appears as a decay in NLMC approach, where zero constraints are imposed outside the target RVE. In our case, the solution at the target RVE becomes independent of oversampling domain size.

Step 3. Substitution in the variational formulation.

In this step, we use u and v expansion in the fine-grid formulation of the problem. In particular, we have

$$\begin{aligned} u &= \phi_m^i U_m^i + \phi_m^{il}\nabla_l U_m^i + \phi_m^{ilp}\nabla_{lp}^2 U_m^i \\ v &= \phi_m^i V_m^i + \phi_m^{il}\nabla_l V_m^i + \phi_m^{ilp}\nabla_{lp}^2 V_m^i. \end{aligned} \tag{15}$$

We substitute and get the following equation (we use matrix notations for ϕ's)

$$\begin{aligned} &\sum_{R_\omega} \frac{|\omega|}{|R_\omega|}\{\int_{R_\omega} \frac{\partial}{\partial t}(\phi_m U_m + \phi_m^l \nabla_l U_m + \phi_m^{lp}\nabla_{lp}^2 U_m)(\phi_n V_n + \phi_n^k \nabla_k V_n + \phi_n^{ks}\nabla_{ks}^2 V_n) \\ &a_{R_\omega}(\phi_m U_m, \phi_n V_n) + a_{R_\omega}(\phi_m U_m, \phi_n^k \nabla_k V_n) + a_{R_\omega}(\phi_m U_m, \phi_n^{ks}\nabla_{ks}^2 V_n) + \\ &a_{R_\omega}(\phi_m^l \nabla_l U_m, \phi_n V_n) + a_{R_\omega}(\phi_m^l \nabla_l U_m, \phi_n^k \nabla_k V_n) + a_{R_\omega}(\phi_m^l \nabla_l U_m, \phi_n^{ks}\nabla_{ks}^2 V_n) + \\ &a_{R_\omega}(\phi_m^{lp}\nabla_{lp}^2 U_m, \phi_n V_n) + a_{R_\omega}(\phi_m^{lp}\nabla_{lp}^2 U_m, \phi_n^k \nabla_k V_n) + a_{R_\omega}(\phi_m^{lp}\nabla_{lp}^2 U_m, \phi_n^{ks}\nabla_{ks}^2 V_n)\} \\ &= \sum_{R_\omega} \frac{|\omega|}{|R_\omega|} \int_{R_\omega} f(\phi_n V_n + \phi_n^k \nabla_k V_n + \phi_n^{ks}\nabla_{ks}^2 V_n). \end{aligned} \tag{16}$$

Our next two steps include using RVE concepts and taking into account that U_i and V_i are smooth functions.

Step 4. Integral localization.

Our next step includes dividing the integral over the coarse partition ω and then using the RVE concept. More precisely, for each integral and a smooth function F, we have

$$\int_D F = \sum_\omega F \approx \sum_\omega \frac{|\omega|}{|R_\omega|} \int_{R_\omega} F. \tag{17}$$

We note that we use only R_ω as the solution in the representative elements near the boundary of the oversampled region ∂R_ω^+ are affected by artificial boundary conditions.

Step 5. Piecesmooth approximation of macroscopic terms.

In this step, the macroscopic terms, U_i and V_i assumed to be smooth functions and the operator A acts only on cell problem solutions. As before (in zero-order equation case), we take the macroscopic variables out of the integrals over R_ω. To demonstrate this step, we consider only two term expansion in (15) writing the integrals over RVE.

More precisely, the terms in the equation (16) have the following forms in R_ω.

$$\begin{aligned}
&\sum_\omega \frac{|\omega|}{|R_\omega|}\Big(\int\limits_{R_\omega} \phi_m\phi_n\Big)\frac{\partial}{\partial t}U_mV_n + \sum_\omega \frac{|\omega|}{|R_\omega|}\Big(\int\limits_{R_\omega} \phi_m\phi_n^k\Big)\frac{\partial}{\partial t}U_m\nabla_k V_n+\\
&\sum_\omega \frac{|\omega|}{|R_\omega|}\Big(\int\limits_{R_\omega} \phi_m^l\phi_n\Big)\frac{\partial}{\partial t}\nabla_l U_mV_n + \sum_\omega \frac{|\omega|}{|R_\omega|}\Big(\int\limits_{R_\omega} \phi_m^l\phi_n^k\Big)\frac{\partial}{\partial t}\nabla_l U_m\nabla_k V_n+\\
&+\sum_\omega \frac{|\omega|}{|R_\omega|}a_{R_\omega}(\phi_m,\phi_n)U_mV_n + \sum_\omega \frac{|\omega|}{|R_\omega|}a_{R_\omega}(\phi_m,\phi_n^k)U_m\nabla_k V_n+\\
&\sum_\omega \frac{|\omega|}{|R_\omega|}a_{R_\omega}(\phi_m^l,\phi_n)\nabla_l U_mV_n + \sum_\omega \frac{|\omega|}{|R_\omega|}a_{R_\omega}(\phi_m^l,\phi_n^k)\nabla_l U_m\nabla_k V_n+\\
&=\sum_\omega \frac{|\omega|}{|R_\omega|}\Big(\int\limits_{R_\omega} f\phi_n\Big)V_n + \sum_\omega \frac{|\omega|}{|R_\omega|}\Big(\int\limits_{R_\omega} f\phi_n^k\Big)\nabla_k V_n.
\end{aligned} \tag{18}$$

In Equation (18), we further take into account that U_i and V_i are smooth functions defined in D and get the following macroscopic equation for U_i (in strong form)

$$A_{nm}\frac{\partial}{\partial t}U_m + B_{nm}U_m + B^i_{nm}\nabla_i U_m - \nabla_k\overline{B}^k_{nm}U_m - \nabla_k(B^{ik}_{nm}\nabla_i U_m) = b_n. \tag{19}$$

Here, we neglect the second, third, and fourth terms in (18). The latter is because ϕ_n^k is of order RVE size, while ϕ_n is of order $O(1)$, in general. Because the coefficients in the operator A have high-contrast properties, we can not neglect these terms. We will remark on this later. The coefficients A's and B's are defined from (18). More precisely,

$$\begin{aligned}
&A_{nm} = \frac{1}{|R_\omega|}\int\limits_{R_\omega}\phi_m\phi_n, \quad b_n = \frac{1}{|R_\omega|}\int\limits_{R_\omega} f\phi_n,\\
&B_{nm} = \frac{1}{|R_\omega|}a_{R_\omega}(\phi_m,\phi_n), \quad B^i_{nm} = \frac{1}{|R_\omega|}a_{R_\omega}(\phi^i_m,\phi_n),\\
&\overline{B}^k_{nm} = \frac{1}{|R_\omega|}a_{R_\omega}(\phi_m,\phi^k_n), \quad B^{ik}_{nm} = \frac{1}{|R_\omega|}a_{R_\omega}(\phi^i_m,\phi^k_n).
\end{aligned} \tag{20}$$

If we use the second-order expansion, the macroscopic equation will have the following form

$$\begin{aligned}
&A_{nm}\frac{\partial}{\partial t}U_m+\\
&B_{nm}U_m + B^i_{nm}\nabla_i U_m + B^{ij}_{nm}\nabla^2_{ij}U_m-\\
&\nabla_k(B^k_{nm}U_m) - \nabla_k(B^{ik}_{nm}\nabla_i U_m) - \nabla_k(B^{ijk}_{nm}\nabla^2_{ij}U_m)+\\
&\nabla^2_{kp}(B^{kp}_{nm}U_m) + \nabla^2_{kp}(B^{ikp}_{nm}\nabla_i U_m) + \nabla^2_{kp}(B^{ijkp}_{nm}\nabla^2_{ij}U_m) = b_n.
\end{aligned} \tag{21}$$

Next, we make several remarks.

First, different terms in the macroscopic equation can have negligible weights. In general, ϕ_k's (the cell solutions accounting for the averages) are of order $O(1)$, while ϕ^n_k's (the cell solutions accounting for the gradients) are of order $O(\epsilon)$, where ϵ is the RVE size (see [22]). For this reason, we have neglected some terms in the time derivative terms and source terms. However, because of high-contrast coefficients, one can not neglect different terms that stem from ϕ_k's or from ϕ^n_k's. In [22], we show that the zero-order terms are important when there is high contrast. More precisely, the reaction terms scale as the inverse of the RVE size. If the effective diffusivity is high, then the reaction and diffusion terms balance each other. Otherwise, one can show that there is no multicontinuum and our macroscopic equations result to single continuum homogenization.

Our second remark is regarding the definition of the continua. Throughout the paper, we assume that ψ_i's are associated with subregions defined apriori. In general, one can use spatial functions for ψ_i, for example, defined via local spectral problems as it is done in nonlocal multicontinua approach or GMsFEM [20,34]. In summary, we formulate conditions that are needed for multicontinuum homogenizatiom.

- We require that the solutions of cell problems (ϕ_m, ϕ^j_m,...) do not depend on oversampling domain sizes, which show that the boundary conditions do not affect the solution in the middle RVE much.
- We require that U_i are smooth functions.

- We need ψ_i to approximate smooth functions in the whole domain D, in some sense. More precisely, we assume that $\|u - \mathcal{P}u\|_{\mathcal{V}(\omega)} \leq C H^{\xi_\omega} \|u - \mathcal{P}u\|_{\mathcal{W}(\omega)}$, for each ω, for some $\xi_\omega > 0$, where $\mathcal{W} \subset \mathcal{V}$. The typical norms for elliptic equations are $\|u\|_{\mathcal{V}(\omega)} = \int_\omega \kappa u^2$ and $\|u\|_{\mathcal{W}(\omega)} = \int_\omega \kappa |\nabla u|^2$.

3.1. Example. A scalar elliptic equation

This example is discussed in [22]. We briefly mention it here. We will focus on multicontinuum expansion, macroscopic equations, and constraints, for simplicity, and do not write down the cell problem equations (cf. (12)). The multicontinuum expansion is $u = \phi_i U_i + \phi_i^m \nabla_m U_i$, where cell solutions have constraints for ϕ_m

$$\int\limits_{R_\omega^p} \phi_m \psi_n^p = \delta_{mn} \int\limits_{R_\omega^p} \psi_n^p \tag{22}$$

and for ϕ_m^l

$$\int\limits_{R_\omega^p} \phi_m^l \psi_n^p = \delta_{mn} \int\limits_{R_\omega^p} (x_l - c_l) \psi_n^p. \tag{23}$$

Note that the equations for ϕ_m and for ϕ_m^l are solved separately.

The macroscopic equations have the following form

$$B_{nm} U_m + B_{nm}^i \nabla_i U_m - \nabla_k (\overline{B}_{nm}^k U_m) - \nabla_k (B_{nm}^{ik} \nabla_i U_m) = b_n. \tag{24}$$

3.2. Comments on error analysis

The analysis of multicontinuum homogenization for elliptic equations can be carried out. We post the results in a separate arxiv document [27]. The proof uses the ideas from NLMC and estimates the difference between U_i and the averaged fine-scale solution defined via $\int u \psi_i$. More precisely, we estimate $\|A^*([U_i] - [\langle u \rangle_i])\|$, where A^* is the homogenized operator, $[U_i]$ is the vector consisting of U_i's, and $\langle u \rangle_i$ is an appropriate average of the fine-grid solution in ith continuum. It was shown that this residual is small. The proof uses the smoothness of U_i and the properties of the cell solutions. Furthermore, the proof assumes regularity for the inverse of A^* to conclude the closness of U_i and $\langle u \rangle_i$. The details can be found in [27].

3.3. Example. A system of elliptic equations

We consider

$$-\frac{\partial}{\partial x_k} (A_{ji}^{kl} \frac{\partial}{\partial x_l} u_i) = f_j. \tag{25}$$

The multicontinuum expansion has the following form

$$u_i = \phi_{mij} U_{mj} + \phi_{mij}^k \nabla_k U_{mj},$$

where the cell problems have the constraints for ϕ_{imn}

$$\int\limits_{R_\omega^p} \phi_{mij} \psi_n^p = \delta_{mn} \delta_{ij} \int\limits_{R_\omega^p} \psi_n^p \tag{26}$$

and for ϕ_{mij}^l

$$\int\limits_{R_\omega^p} \phi_{mij}^l \psi_n^p = \delta_{mn} \delta_{ij} \int\limits_{R_\omega^p} (x_l - c_l) \psi_n^p. \tag{27}$$

For example, for two equations, we have

$$\begin{bmatrix} u_1 \\ u_2 \end{bmatrix} = \begin{bmatrix} \phi_{j11} & \phi_{j12} \\ \phi_{j21} & \phi_{j22} \end{bmatrix} \begin{bmatrix} U_{j1} \\ U_{j2} \end{bmatrix} + \begin{bmatrix} \phi_{j11}^m & \phi_{j12}^m \\ \phi_{j21}^m & \phi_{j22}^m \end{bmatrix} \begin{bmatrix} \nabla_m U_{j1} \\ \nabla_m U_{j2} \end{bmatrix}. \tag{28}$$

The constraints are the following

$$\int\limits_{R_\omega^p} \begin{bmatrix} \phi_{m11} \\ \phi_{m21} \end{bmatrix} \psi_n^p = \delta_{mn} \begin{bmatrix} 1 \\ 0 \end{bmatrix} \int\limits_{R_\omega^p} \psi_n^p, \quad \int\limits_{R_\omega^p} \begin{bmatrix} \phi_{m12} \\ \phi_{m22} \end{bmatrix} \psi_n^p = \delta_{mn} \begin{bmatrix} 0 \\ 1 \end{bmatrix} \int\limits_{R_\omega^p} \psi_n^p, \tag{29}$$

$$\int\limits_{R_\omega^p} \begin{bmatrix} \phi_{m11}^k \\ \phi_{m21}^k \end{bmatrix} \psi_n^p = \delta_{mn} \begin{bmatrix} 1 \\ 0 \end{bmatrix} \int\limits_{R_\omega^p} (x_k - c_k)\psi_n^p,$$
$$\int\limits_{R_\omega^p} \begin{bmatrix} \phi_{m12}^k \\ \phi_{m22}^k \end{bmatrix} \psi_n^p = \delta_{mn} \begin{bmatrix} 0 \\ 1 \end{bmatrix} \int\limits_{R_\omega^p} (x_k - c_k)\psi_n^p. \tag{30}$$

The macroscopic equations have the following form

$$B_{ijnm}U_{jm} + B_{ijnm}^l \nabla_l U_{jm} - \nabla_k (B_{ijnm}^k U_{jm}) - \nabla_k (B_{ijnm}^{lk} \nabla_l U_{jm}) = b_{in}, \tag{31}$$

where

$$B_{ijnm} = a_{R_\omega}(\phi_{mri}, \phi_{ntj}), \quad B_{ijnm}^l = a_{R_\omega}(\phi_{mri}, \phi_{ntj}^l)$$
$$B_{ijnm}^{lk} = a_{R_\omega}(\phi_{mri}^l, \phi_{ntj}^k), \quad b_{in} = \int\limits_{R_\omega} f_r \phi_{nri}, \tag{32}$$

where

$$a_{R_\omega}(u, v) = \int\limits_{R_\omega} A_{ji}^{kl} \frac{\partial}{\partial x_l} u_i \frac{\partial}{\partial x_k} v_j.$$

It can be shown that the second and third terms cancel each other and the scaling of B_{nm} is of order $1/\epsilon^2$, where ϵ is RVE size. Because of high contrast, this term can balance with the diffusion term.

3.4. Mixture theory and its relation

Here, we briefly note that one can also derive general multicontinuum equations using mixture theory [30,33,28]; however, precise micro and macro relations can not be derived from this theory. Mixture theory specifies several model classes [28]. One that is suitable for our models is Class II, where N balances of mass for N components of the mixture and also N balances of linear momentum for N components of mixture are formulated. In this case, the equations have the following form

$$\frac{\partial \rho_i}{\partial t} + div(\rho_i v_i) = m_i, \quad \sum_i m_i = 0,$$
$$\frac{\partial \rho_i v_i}{\partial t} + div(\rho_i v_i \otimes v_i) = div(\mathcal{T}_i) + \mathcal{Q}_i + m_i v_i, \quad \sum_i (\mathcal{Q}_i + m_i v_i) = 0. \tag{33}$$

Here, we use a simplified formulation from [28], and use the notations from [28], where ρ_i is the density of ith component, v_i is the velocity, m_i is the exchange terms for mass conservation, $\mathcal{T}_i$ is the stress tensor, and $\mathcal{Q}_i$ is the exchange terms for momentum.

To derive a multicontinuum equations, we consider solid and two fluid continua mixture. For momentum equations, we have (ignoring gravity)

$$\frac{\partial \rho_1^f v_1^f}{\partial t} + div(\rho_1^f v_1^f \otimes v_1^f) = div(\mathcal{T}_1^f) + \mathcal{Q}_1^f,$$
$$\frac{\partial \rho_2^f v_2^f}{\partial t} + div(\rho_2^f v_2^f \otimes v_2^f) = div(\mathcal{T}_2^f) + \mathcal{Q}_2^f,$$
$$\frac{\partial \rho^s v^s}{\partial t} + div(\rho^s v^s \otimes v^s) = div(\mathcal{T}_s) + \mathcal{Q}^s, \tag{34}$$

where $\mathcal{Q}^s = -\mathcal{Q}_1^f - \mathcal{Q}_2^f$, s denotes the solid and f denotes the fluid. It is assumed that $v^s \approx 0$, $\mathcal{T}_i^f = p_i I$, $i = 1, 2$, $\mathcal{Q}_i^f = \kappa_i^{-1} v_i$, and the flow is steady-state and slow. In the mass conservation equations,

$$\frac{\partial \rho_1^f}{\partial t} + div(\rho_1^f v_1^f) = m_1^f,$$
$$\frac{\partial \rho_2^f}{\partial t} + div(\rho_2^f v_2^f) = m_2^f,$$
$$\frac{\partial \rho^s}{\partial t} + div(\rho^s v^s) = m^s. \tag{35}$$

We have $v^s \approx 0$, $m^s \approx 0$, and take

$$m_1^f = \alpha \rho_1^f (p_2 - p_1)$$
$$m_2^f = \alpha \rho_2^f (p_1 - p_2). \tag{36}$$

The resulting equations have the form of multicontinuum equations (24).

4. First-order mixed system

We consider a first-order mixed system as an example of a system, where the variables are coupled.

$$\begin{aligned} \kappa^{-1} v + \nabla u &= 0 \\ div(v) &= f. \end{aligned} \tag{37}$$

This equation is a non-symmetric system with the solution vector (v, u) and the operator

$$A = \begin{bmatrix} \kappa^{-1} & \nabla \\ div & 0 \end{bmatrix}. \tag{38}$$

The local cell problems and constraints require special attention to avoid the boundary condition influence. We consider the derivation of macroscopic equations. In general, as before, one can use various constraints and derive various macroscopic equations.

We consider piecewise constant velocity and piecewise linear type pressure approximations at the RVE level. We use different notations because differing notations for variables. In this case, we have the following expansion

$$\begin{aligned} v_s &= \phi^{vu}_{is} U_i + \phi^{vu}_{ism} \nabla_m U_i + \phi^{vv}_{isk} V_{ik} \\ u &= \phi^{uu}_{i} U_i + \phi^{uu}_{im} \nabla_m U_i + \phi^{uv}_{ik} V_{ik}. \end{aligned} \tag{39}$$

Here, i refers to the continua, (ϕ^{uv}, ϕ^{uu}) represents the cell solutions with zero constraints on v and (ϕ^{vu}, ϕ^{vv}) represents cell solutions with zero constraints on u (see Section 5, (48)-(50)).

We multiple the mixed system (37) by

$$\begin{bmatrix} \phi^{vu}_j Q_j + \phi^{vu}_{jl} \nabla_l Q_j \\ \phi^{uu}_j Q_j + \phi^{uu}_{jl} \nabla_l Q_j \end{bmatrix} \tag{40}$$

and sum up the equations (use vector notations for simplicity)

$$\begin{aligned} &\int_{R_\omega} (\phi^{vu}_j Q_j + \phi^{vu}_{jl} \nabla_l Q_j) \kappa^{-1} (\phi^{vu}_i U_i + \phi^{vu}_{im} \nabla_m U_i + \phi^{vv}_i V_i) \\ &+ \int_{R_\omega} (\phi^{vu}_j Q_j + \phi^{vu}_{jl} \nabla_l Q_j) \nabla (\phi^{uu}_i U_i + \phi^{uu}_{im} \nabla_m U_i + \phi^{uv}_i V_i) \\ &+ \int_{R_\omega} div(\phi^{vu}_i U_i + \phi^{vu}_{im} \nabla_m U_i + \phi^{vv}_i V_i)(\phi^{uu}_j Q_j + \phi^{uu}_{jl} \nabla_l Q_j) \\ &= \int_{R_\omega} f(\phi^{uu}_j Q_j + \phi^{uu}_{jl} \nabla_l Q_j). \end{aligned} \tag{41}$$

In the global form, the equation has the form

$$\alpha^u_{ij} U_i + \alpha^u_{ijm} \nabla_m U_i - \nabla_m (\overline{\alpha}^u_{ijm} U_i) - \nabla_n (\alpha^u_{ijnm} \nabla_m U_i) + \beta^u_{ji} V_i + \beta^u_{jim} \nabla_m V_i = f^u_j. \tag{42}$$

In our numerical simulations, we observe that the sum of two convection terms (the second and third terms in the equation) is small and can be neglected. This is because In our calculations, we drop some of the terms depending on the relative scalings of ϕ's and their gradients.

Next, we multiply the system (37) by

$$\begin{bmatrix} \phi^{vv}_j Q_j \\ \phi^{uv}_j Q_j \end{bmatrix} \tag{43}$$

and sum up (use vector notations for simplicity)

$$\begin{aligned}
&\int_{R_\omega} \phi_j^{vv} Q_j \kappa^{-1}(\phi_i^{vu} U_i + \phi_{im}^{vu} \nabla_m U_i + \phi_i^{vv} V_i) \\
&+ \int_{R_\omega} \phi_j^{vv} Q_j \nabla(\phi_i^{uu} U_i + \phi_{im}^{uu} \nabla_m U_i + \phi_i^{uv} V_i) \\
&+ \int_{R_\omega} div(\phi_i^{vu} U_i + \phi_{im}^{vu} \nabla_m U_i + \phi_i^{vv} V_i) \phi_j^{uv} Q_j \\
&= \int_{R_\omega} f \phi_j^{uv} Q_j.
\end{aligned} \tag{44}$$

In the global form, the equation has the form

$$\alpha_{ij}^v U_i + \alpha_{ijm}^v \nabla_m U_i + \beta_{ji}^v V_i = f_j^v. \tag{45}$$

In our numerical simulations, we observe that α_{ij}^v is small and can be neglected.

In general, one can choose a more general representation of the velocity via piecewise linear functions and obtain general models with higher order derivatives.

Note that the polynomial constraints in the approximation of velocity and pressures in (39) is for homogenization and is not related to stable polynomial approximation in finite element methods.

5. Numerical example

In this section, we will present some numerical examples to demonstrate the performance of the method in a mixed formulation. Here, we propose the following local problems for velocity v and pressure u in the equation

$$\begin{aligned}
\kappa^{-1} v + \nabla u &= 0 \\
div(v) &= q.
\end{aligned} \tag{46}$$

Next, we describe the local solutions for velocity and pressure. We will only write down the constraints, the formulation of the local problem follows from equations (12) and (13). For the velocity constraints, we impose an intermediate domain R_ω^V, where R_ω^V is a subset of R_ω^+ and contains R_ω. Moreover, we assume that R_ω^V consists of R_ω^p, where p is a numeration of local domains, one of them being R_ω. We remind that the local solution has the following matrix form.

$$\begin{bmatrix} u \\ v_s \end{bmatrix} = \begin{bmatrix} \phi_i^{uu} & \phi_{im}^{uu} & \phi_{ik}^{uv} \\ \phi_{is}^{vu} & \phi_{ism}^{vu} & \phi_{isk}^{vv} \end{bmatrix} \begin{bmatrix} U_i \\ \nabla_m U_i \\ V_{ik} \end{bmatrix} \tag{47}$$

The local constraints for ϕ's are imposed column by column. The constraints are the following

$$\begin{aligned}
&\int_{R_\omega^p} \phi_i^{uu} \psi_j = \delta_{ij} \int_{R_\omega^p} \psi_j, \ \forall R_\omega^p \subset R_\omega^+, \\
&\int_{R_\omega^p} \phi_{is}^{vu} \psi_j = 0, \ \forall R_\omega^p \subset R_\omega^V,
\end{aligned} \tag{48}$$

and

$$\begin{aligned}
&\int_{R_\omega^p} \phi_{im}^{uu} \psi_j = \delta_{ij} \int_{R_\omega^p} (x_m - c_m) \psi_j, \ \forall R_\omega^p \subset R_\omega^+, \\
&\int_{R_\omega^p} \phi_{ism}^{vu} \psi_j = 0, \ \forall R_\omega^p \subset R_\omega^V,
\end{aligned} \tag{49}$$

and

$$\begin{aligned}
&\int_{R_\omega^p} \phi_{ik}^{uv} \psi_j = 0, \ \forall R_\omega^p \subset R_\omega^+, \\
&\int_{R_\omega^p} \phi_{isk}^{vv} \psi_j = \delta_{ij} \delta_{sk} \int_{R_\omega^p} \psi_j, \ \forall R_\omega^p \subset R_\omega^V.
\end{aligned} \tag{50}$$

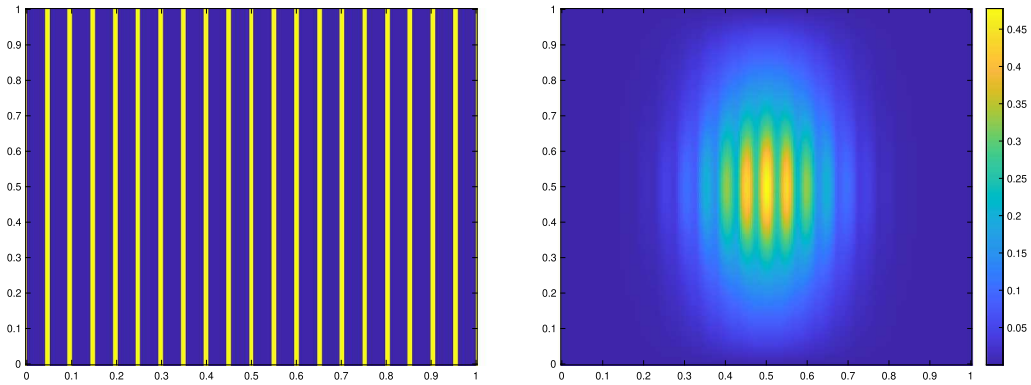

Fig. 2. Case 1. Left: Parameter κ. Right: Reference solution. (For interpretation of the colors in the figure(s), the reader is referred to the web version of this article.)

Table 1
Error comparison for Case 1.

H	ϵ	$e_2^{(1)}$	$e_2^{(2)}$	H	ϵ	$e_2^{(1)}$	$e_2^{(2)}$
1/10	1/10	27.19%	6.21%	1/10	1/10	27.19%	6.21%
1/20	1/20	11.63%	1.19%	1/10	1/20	12.79%	2.43%
1/40	1/40	3.25%	0.88%	1/10	1/40	6.32%	1.70%

In the calculations of macroscopic domains, we use another intermediate domain R_ω^I, which is a subset of R_ω^+ and contains R_ω^V. The local expansion is given by (39).

In the first example, we consider the layered medium depicted on Fig. 2. The permeability field κ has a period denoted by ϵ. We denote the low conductivity region and the high conductivity region of κ by Ω_1 and Ω_2, respectively. The source term f and conductivity κ are as follows

$$f(x) = \begin{cases} 1000 \min\{\kappa\} e^{-40|(x-0.5)^2+(y-0.5)^2|} & x \in \Omega_1 \\ e^{-40|(x-0.5)^2+(y-0.5)^2|} & x \in \Omega_2 \end{cases}$$

and

$$\kappa(x) = \begin{cases} \dfrac{\epsilon}{10000} & x \in \Omega_1 \\ \dfrac{1}{100\epsilon} & x \in \Omega_2 \end{cases}$$

We divide the computational domain Ω into $M \times M$ coarse grid. The coarse mesh size H is defined as $H = 1/M$. We consider the whole coarse grid element as an RVE for the corresponding coarse element. The oversampling RVE R_ω^+ (or ω^+) for each coarse RVE ω is defined as an extension of K (target coarse block) by l layers of coarse grid element, where l will be changed in simulations.

We define the relative L^2- error in Ω_1 and the relative L^2- error in Ω_2 by

$$(e_2^{(i)})^2 = \frac{\sum_K |\frac{1}{|K|}\int_K U_i - \frac{1}{|K \cap \Omega_i|}\int_{K\cap\Omega_i} u|^2}{\sum_K |\frac{1}{K \cap \Omega_i}\int_{K\cap\Omega_i} u|^2}.$$

K denotes the RVE, which is taken to be ω.

For the first case, we take the fine-mesh size to be $H\epsilon$. We present $e_2^{(i)}$ in Table 1. First, we observe that the proposed approach provides an accurate approximation of the averaged solution as we decrease the mesh size. In Fig. 3, we depict upscaled solutions and corresponding averaged fine-scale solutions. We observe that these solutions are very close. In the first table, we decrease the coarse-mesh size and the period size. In standard numerical homogenization methods, this gives a resonance error (stagnating errors). Here, by choosing an appropriate number of layers, we observe that the error remains small. In the second table, we fix the mesh size and decrease ϵ. Our theoretical results suggest that the error is of order H. In this case, the error will decrease as it reaches of order H and then stagnates.

For the second case, we change the permeability field to the one shown in Fig. 4. We present $e_2^{(i)}$ in Table 2. Again, we observe that the proposed approach provides an accurate approximation of the averaged solution as we decrease the mesh size. In Fig. 5, we depict upscaled solutions and corresponding averaged fine-scale solutions. We observe a good agreement between coarse- and fine-grid solutions. In the first table, we decrease the coarse-mesh size and the period size at the same time. We observe that the total error decreases as the mesh size decreases. Note that the individual continuum error may not decrease. Our theoretical results

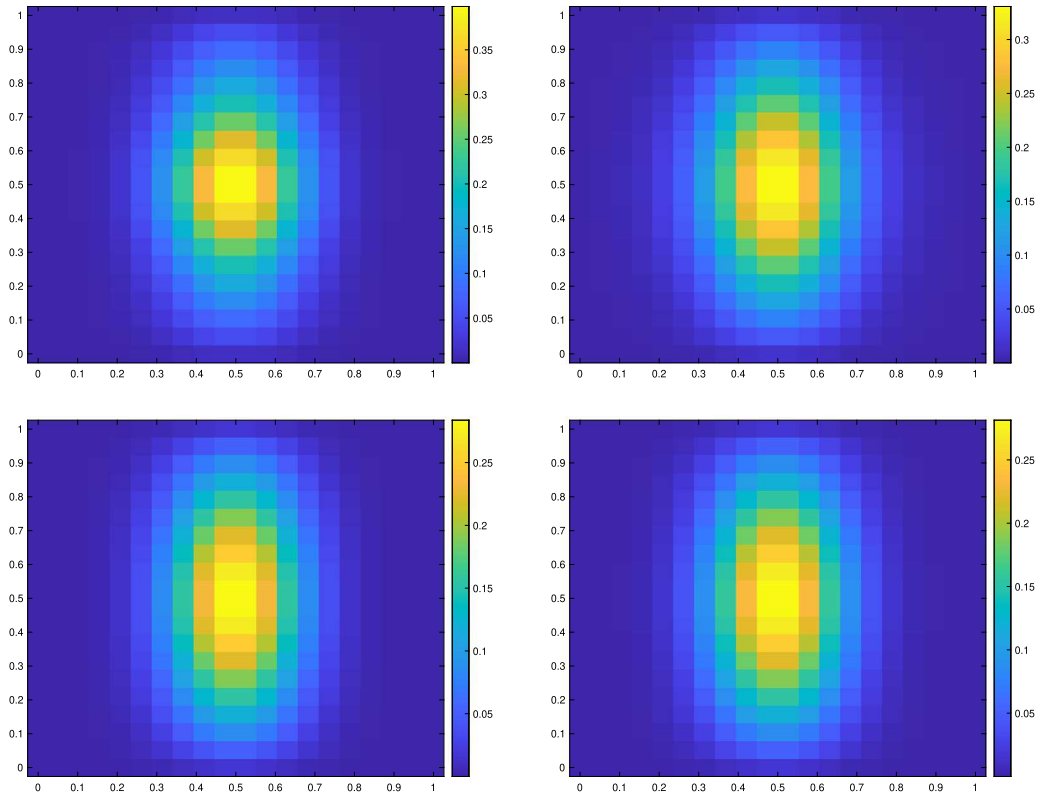

Fig. 3. Case 1. Top-Left: reference average solution in Ω_1. Top-Right: homogenized average solution in Ω_1. Bottom-Left: reference average solution in Ω_2. Bottom-Right: homogenized average solution in Ω_2.

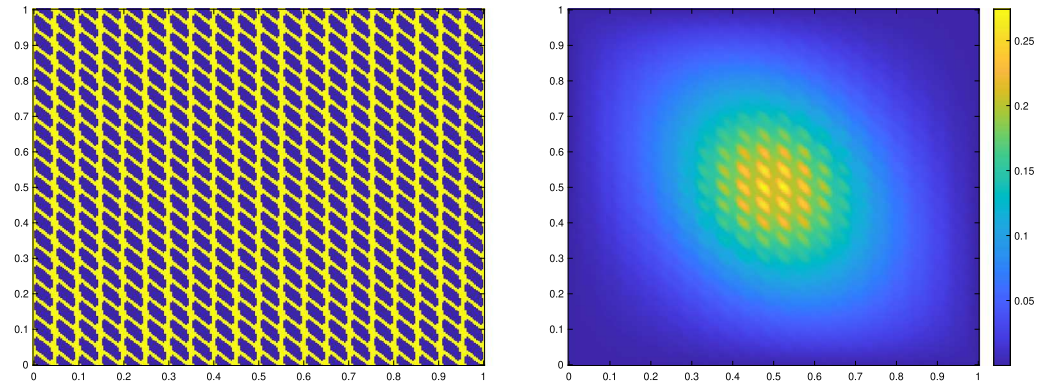

Fig. 4. Case 2. Left: Parameter κ. Right: reference solution.

Table 2
Error comparison for Case 2.

H	ϵ	$e_2^{(1)}$	$e_2^{(2)}$	H	ϵ	$e_2^{(1)}$	$e_2^{(2)}$
1/10	1/10	11.74%	1.61%	1/10	1/10	11.74%	1.61%
1/20	1/20	4.18%	0.97%	1/10	1/20	9.12%	6.13%
1/40	1/40	1.86%	1.08%	1/10	1/40	8.05%	7.27%

suggest that the total error will decrease. Here, by choosing an appropriate number of layers, we observe that the error remains small. In the second table, we fix the mesh size and decrease ϵ. Our theoretical results suggest that the error is of order H. In this case, the error does not decrease as the decrease of ϵ does not affect the error because the error is dominated by H.

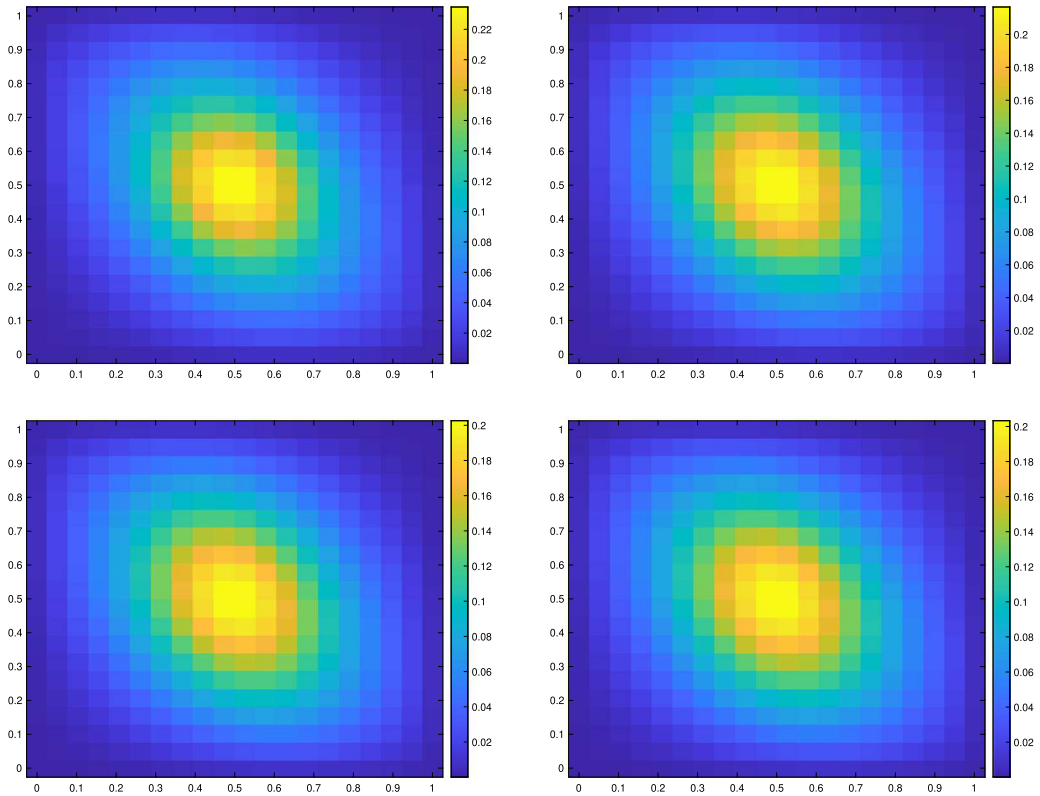

Fig. 5. Case 2. Top-Left: reference average solution in Ω_1. Top-Right: homogenized average solution in Ω_1. Bottom-Left: reference average solution in Ω_2. Bottom-Right: homogenized average solution in Ω_2.

6. Conclusions

In this paper, we propose a general framework for multicontinuum homogenization. The method introduces several macroscopic variables at each macroscale point using characteristic functions associated with subdomains. The homogenization expansion is written using macroscale variables and associated local cell problems. The local cell problems are formulated as constraint problems in oversampled regions. This is not an easy task, in general, since the constraints are formulated in a spatially localized fashion. We present an example of a mixed formulation of the elliptic equation, where we use some special formulations for cell problems. The proposed general framework shows that one can obtain various macroscale equations. We briefly discuss the relation to mixture theories.

CRediT authorship contribution statement

E. Chung: Conceptualization, Writing – original draft, Writing – review & editing. **Y. Efendiev:** Conceptualization, Formal analysis, Writing – original draft, Writing – review & editing. **J. Galvis:** Conceptualization, Writing – original draft, Writing – review & editing. **W.T. Leung:** Conceptualization, Writing – original draft, Writing – review & editing.

Declaration of competing interest

The authors declare that they have no known competing financial interests or personal relationships that could have appeared to influence the work reported in this paper.

Data availability

No data was used for the research described in the article.

Acknowledgements

The research of EC is partially supported by the Hong Kong RGC General Research Fund (Projects: 14305222 and 14304021). YE would like to thank the partial support from NSF 2208498. WTL is supported by Early Career Award, Research Grant Council, Project Number: 21307223.

References

[1] E. Abreu, C. Díaz, J. Galvis, A convergence analysis of generalized multiscale finite element methods, J. Comput. Phys. 396 (2019) 303–324.
[2] E. Abreu, C. Diaz, J. Galvis, J. Pérez, On the conservation properties in multiple scale coupling and simulation for Darcy flow with hyperbolic-transport in complex flows, Multiscale Model. Simul. 18 (4) (2020) 1375–1408.
[3] E.C. Aifantis, Continuum basis for diffusion in regions with multiple diffusivity, J. Appl. Phys. 50 (3) (1979) 1334–1338.
[4] G. Allaire, Homogenization and two-scale convergence, SIAM J. Math. Anal. 23 (6) (1992) 1482–1518.
[5] M. Alotaibi, H. Chen, S. Sun, Generalized multiscale finite element methods for the reduced model of Darcy flow in fractured porous media, J. Comput. Appl. Math. 413 (2022) 114305.
[6] R. Altmann, P. Henning, D. Peterseim, Numerical homogenization beyond scale separation, Acta Numer. 30 (2021) 1–86.
[7] T. Arbogast, J. Douglas Jr, U. Hornung, Derivation of the double porosity model of single phase flow via homogenization theory, SIAM J. Math. Anal. 21 (4) (1990) 823–836.
[8] N.S. Bakhvalov, G. Panasenko, Homogenisation: Averaging Processes in Periodic Media: Mathematical Problems in the Mechanics of Composite Materials, vol. 36, Springer Science & Business Media, 2012.
[9] G.I. Barenblatt, I.P. Zheltov, I. Kochina, Basic concepts in the theory of seepage of homogeneous liquids in fissured rocks [strata], J. Appl. Math. Mech. 24 (5) (1960) 1286–1303.
[10] A. Bedford, M. Stern, A multi-continuum theory for composite elastic materials, Acta Mech. 14 (2) (1972) 85–102.
[11] A. Bensoussan, J.-L. Lions, G. Papanicolaou, Asymptotic Analysis for Periodic Structures, vol. 374, American Mathematical Soc., 2011.
[12] X. Blanc, C. Le Bris, Homogenization Theory for Multiscale Problems: An Introduction, vol. 21, Springer Nature, 2023.
[13] F. Brezzi, On the Existence, Uniqueness and Approximation of Saddle-Point Problems Arising from Lagrangian Multipliers, Publications des Séminaires de Mathématiques et Informatique de Rennes, vol. S4, 1974, pp. 1–26.
[14] R. Bunoiu, C. Timofte, Upscaling of a Diffusion Problem with Interfacial Flux Jump Leading to a Modified Barenblatt Model, 2019.
[15] Z. Chai, B. Yan, J. Killough, Y. Wang, An efficient method for fractured shale reservoir history matching: the embedded discrete fracture multi-continuum approach, J. Pet. Sci. Eng. 160 (2018) 170–181.
[16] E. Chung, Y. Efendiev, T.Y. Hou, Multiscale Model Reduction: Multiscale Finite Element Methods and Their Generalizations, Springer, 2023.
[17] E.T. Chung, Y. Efendiev, T. Hou, Adaptive multiscale model reduction with generalized multiscale finite element methods, J. Comput. Phys. 320 (2016) 69–95.
[18] E.T. Chung, Y. Efendiev, W.T. Leung, Constraint energy minimizing generalized multiscale finite element method, Comput. Methods Appl. Mech. Eng. 339 (2018) 298–319.
[19] L. Contreras, D. Pardo, E. Abreu, J. Muñoz-Matute, C. Diaz, J. Galvis, An exponential integration generalized multiscale finite element method for parabolic problems, J. Comput. Phys. 479 (2023) 112014.
[20] Y. Efendiev, J. Galvis, T. Hou, Generalized multiscale finite element methods (GMsFEM), J. Comput. Phys. 251 (2013) 116–135.
[21] Y. Efendiev, T. Hou, Multiscale Finite Element Methods: Theory and Applications, Surveys and Tutorials in the Applied Mathematical Sciences, vol. 4, Springer, New York, 2009.
[22] Y. Efendiev, W.T. Leung, Multicontinuum homogenization and its relation to nonlocal multicontinuum theories, J. Comput. Phys. 474 (2023) 111761.
[23] J. Fish, Practical Multiscaling, John Wiley & Sons, 2013.
[24] T. Hou, X. Wu, A multiscale finite element method for elliptic problems in composite materials and porous media, J. Comput. Phys. 134 (1997) 169–189.
[25] D. Ieşan, A theory of mixtures with different constituent temperatures, J. Therm. Stresses 20 (2) (1997) 147–167.
[26] P. Jenny, S. Lee, H. Tchelepi, Multi-scale finite volume method for elliptic problems in subsurface flow simulation, J. Comput. Phys. 187 (2003) 47–67.
[27] W.T. Leung, Some convergence analysis for multicontinuum homogenization, arXiv preprint, arXiv:2401.12799, 2024.
[28] J. Malek, O. Soucek, Theory of Mixtures, 2020.
[29] H. Owhadi, L. Zhang, Metric-based upscaling, Commun. Pure Appl. Math. 60 (2007) 675–723.
[30] K.R. Rajagopal, L. Tao, Mechanics of Mixtures, vol. 35, World Scientific, 1995.
[31] L. Rubinšteın, On a question about the propagation of heat in heterogeneous media, Izv. Akad. Nauk SSSR, Ser. Geogr. Geofiz. 12 (1948) 27–45 (Russian).
[32] R. Showalter, N. Walkington, Micro-structure models of diffusion in fissured media, J. Math. Anal. Appl. 155 (1) (1991) 1–20.
[33] C. Truesdell, I.-S. Liu, I. Müller, Thermodynamics of Mixtures of Fluids, Springer, 1984.
[34] M. Vasilyeva, E.T. Chung, W.T. Leung, V. Alekseev, Nonlocal multicontinuum (nlmc) upscaling of mixed dimensional coupled flow problem for embedded and discrete fracture models, GEM Int. J. Geomath. 10 (2019) 1–23.